Superantigens promote *Staphylococcus aureus* bloodstream infection by eliciting pathogenic interferon-gamma production

Stephen W. Tuffs[a], Mariya I. Goncheva[a], Stacey X. Xu[a], Heather C. Craig[a], Katherine J. Kasper[a], Joshua Choi[a], Ronald S. Flannagan[a], Steven M. Kerfoot[a], David E. Heinrichs[a], and John K. McCormick[a,b,1]

[a]Department of Microbiology and Immunology, University of Western Ontario, London, ON N6A 5C1, Canada; and [b]Lawson Health Research Institute, London, ON N6A 4V2, Canada

Edited by Philippa Marrack, Department of Immunology and Genomic Medicine, National Jewish Health, Denver, CO; received August 30, 2021; accepted January 7, 2022

Staphylococcus aureus **is a foremost bacterial pathogen responsible for a vast array of human diseases. Staphylococcal superantigens (SAgs) constitute a family of exotoxins from *S. aureus* that bind directly to major histocompatibility complex (MHC) class II and T cell receptors to drive extensive T cell activation and cytokine release. Although these toxins have been implicated in serious disease, including toxic shock syndrome, the specific pathological mechanisms remain unclear. Herein, we aimed to elucidate how SAgs contribute to pathogenesis during bloodstream infections and utilized transgenic mice encoding human MHC class II to render mice susceptible to SAg activity. We demonstrate that SAgs contribute to *S. aureus* bacteremia by massively increasing bacterial burden in the liver, and this was mediated by $CD4^+$ T cells that produced interferon gamma (IFN-γ) to high levels in a SAg-dependent manner. Bacterial burdens were reduced by blocking IFN-γ, phenocopying SAg-deletion mutant strains, and inhibiting a proinflammatory response. Infection kinetics and flow cytometry analyses suggested that this was a macrophage-driven mechanism, which was confirmed through macrophage-depletion experiments. Experiments in human cells demonstrated that excessive IFN-γ allowed *S. aureus* to replicate efficiently within macrophages. This indicates that SAgs promote bacterial survival by manipulating the immune response to inhibit effective clearing of *S. aureus*. Altogether, this work implicates SAg toxins as critical therapeutic targets for preventing persistent or severe *S. aureus* disease.**

Staphylococcus aureus | superantigen | interferon gamma | macrophage

Staphylococcus aureus is an important bacterial pathogen that can exist as a harmless commensal. Yet once primary barriers have been breached, this pathobiont also has the propensity to cause an extraordinary range of superficial, invasive, and toxin-mediated diseases (1). This spectrum of disease can range from relatively simple soft-tissue infection to pneumonia or bacteremia that may lead to life-threatening sepsis (1, 2). *S. aureus* is one of the most common causes of sepsis and carries a high mortality rate of 20 to 40% that can double in the context of septic shock (2, 3). Widespread drug resistance, including both hospital- and community-associated methicillin-resistant *S. aureus* (MRSA), has further exacerbated treatment challenges with this important pathogen (4).

Key to the success of *S. aureus* as a pathogen is a vast array of virulence factors encoded both within the chromosome and on mobile genetic elements. These factors fall into several functional classes including adhesion factors (e.g., fibronectin-binding proteins A and B [FnbpA and FnbpB]) (5, 6), immunomodulatory proteins (e.g., staphylococcal protein A [Spa] or chemotaxis inhibitor protein of *Staphylococcus* [CHIPS]) (7), cytolytic toxins (e.g., alpha-hemolysin [Hla]) (8, 9), and superantigens (SAgs). The SAg family in *S. aureus* consists of at least 26 different paralogues that function by cross-linking major histocompatibility complex (MHC) class II molecules with the variable region of the T cell receptor (TCR) β-chain (Vβ); the unconventional interaction with these two key immune receptors occurs irrespective of the cognate antigen and results in the aberrant and widespread activation of T cells followed by proinflammatory cytokine release (10).

SAgs are the etiological agent of toxic shock syndrome, in which T cell activation caused by SAgs released from *S. aureus* triggers a systemic "cytokine storm" that can lead to hypotension and multiple organ failure and, in some cases, death. SAg activity has also been implicated in a number of other serious diseases including endocarditis, pneumonia, and bacteremia (11). Historically, it has been difficult to model the biological functions of SAg activity in vivo, as conventional murine strains are highly insensitive to these toxins. As a result, much of the pathogenesis work related to SAgs has been performed in rabbits, which are inherently sensitive to SAg activity (12–14). However, we have demonstrated that transgenic mice expressing the human leukocyte antigen (HLA)-DR4 are significantly more sensitive to SAg activity (15, 16). This allowed us to determine that staphylococcal SAgs are important during bloodstream infections leading to increased bacterial burdens within the liver (15).

Significance

Since their discovery over 30 y ago, it has become clear that the superantigens (SAgs) are important virulence factors produced during severe *Staphylococcus aureus*–mediated disease including bacteremia. However, until the current study, it was unclear how these toxins manipulated the immune system to promote infection. Here, we have demonstrated that the SAgs can target a critical immune signaling molecule (interferon gamma), inducing overproduction that promotes bacterial survival by subverting the ability of macrophages to be able to kill the pathogen. This highlights SAg activity as a critical target for antistaphylococcal therapy to mitigate the impact of severe *S. aureus* disease.

Author contributions: S.W.T., M.I.G., S.X.X., H.C.C., K.J.K., R.S.F., S.M.K., D.E.H., and J.K.M. designed research; S.W.T., M.I.G., S.X.X., H.C.C., K.J.K., J.C., and R.S.F. performed research; S.W.T., S.X.X., and K.J.K. contributed new reagents/analytic tools; S.W.T., M.I.G., S.X.X., H.C.C., K.J.K., R.S.F., S.M.K., D.E.H., and J.K.M. analyzed data; and S.W.T. and J.K.M. wrote the paper.

The authors declare no competing interest.

This article is a PNAS Direct Submission.

[1]To whom correspondence may be addressed. Email: john.mccormick@uwo.ca.

This article contains supporting information online at http://www.pnas.org/lookup/suppl/doi:10.1073/pnas.2115987119/-/DCSupplemental.

Published February 14, 2022.

In the current study, we deployed targeted antibody depletion protocols that demonstrated, during bloodstream infection, that SAgs target $CD4^+$ T cells to produce pathogenic levels of the key cytokine interferon gamma (IFN-γ). IFN-γ promoted enhanced disease severity and bacterial burden in the liver, and excess IFN-γ levels during infection appeared to perturb liver macrophage activity to promote the survival of *S. aureus*.

Results

Transgenic HLA-DR4 C57BL/6 Mice Are Sensitive to SAgs Staphylococcal Enterotoxin B and Staphylococcal Enterotoxin C Activity and Can Be Used to Model *S. aureus* Bacteremia. Previously, we demonstrated that *S. aureus* burden is promoted during murine bloodstream infections by the SAgs staphylococcal enterotoxin A (SEA) and staphylococcal enterotoxin-like W (SElW); however, the mechanism remained uncharacterized (15, 17). In the current study, we first utilized strain COL, a well-studied MRSA isolate from clonal complex (CC) 8 that produces the SAg staphylococcal enterotoxin B (SEB) (18). Splenocyte analysis from C57BL/6 (B6) or transgenic HLA-DR4 C57BL/6 (DR4-B6) animals identified that T cell activation (measured by the production of IL-2) to titrating doses of SEB was orders of magnitude more active on spleen cells from the DR4-B6 animals compared to conventional B6 mice (Fig. 1*A*). In addition, analysis of stimulated splenocytes using flow cytometry analysis demonstrated a massive expansion of $V\beta8^+$ T cells, the major T cell targets of SEB in mice (19) (Fig. 1*B*). These cells represent ∼20% of the T cell repertoire in the DR4-B6 animals, and the majority of these were activated by SEB as measured by the up-regulation of CD25 (Fig. 1*B*). Together, these data demonstrate that, compared to conventional B6 mice, DR4-B6 mice are highly sensitive to SEB activity and can be used for the analysis of SEB activity in vivo.

To determine if SEB contributed to pathogenicity in murine bacteremia, we infected B6 and DR4-B6 animals with *S. aureus* COL via tail-vein injection. We found that wild-type *S. aureus* COL was significantly more virulent in DR4-B6 mice with a much higher bacterial burden found in the liver and kidneys when compared to the B6 background (Fig. 1*C*). This was due to SEB activity, as the bacterial burden of the SEB-null mutant (COL Δ*seb*) essentially phenocopied the data obtained from the B6 animals. Importantly, this phenotype could be complemented with COL Δ*seb* containing pCM29::*seb* (Fig. 1 *C* and *D*). These data clearly demonstrate that SEB contributes to the pathogenicity of *S. aureus* COL during bloodstream infection.

To determine if additional SAgs other than SEB could also contribute to bacteremia, we expanded our analysis to include *S. aureus* MW2, a CC1 MRSA isolate that produces staphylococcal enterotoxin C (SEC) (20, 21). SEC is phylogenetically similar to SEB and has a similar Vβ activation profile in humans (10, 21). We successfully deleted the SEC gene in *S. aureus* MW2 and were able to complement the gene in trans (*SI Appendix*, Fig. S1). Like *S. aureus* COL, we found a significant increase in bacterial burden in the liver and kidneys in DR4-B6 animals compared to the B6 mice when infected with MW2 (Fig. 1*E*). Furthermore, deletion of *sec* from MW2 resulted in a significant reduction in bacterial burden and liver pathology (Fig. 1 *E* and *F*). These data indicate that both SEB and SEC produced from different *S. aureus* backgrounds can contribute to the pathogenesis of experimental bloodstream infection and that SAg-sensitive DR4-B6 mice are suitable for modeling SAg activity in the context of live *S. aureus* infection.

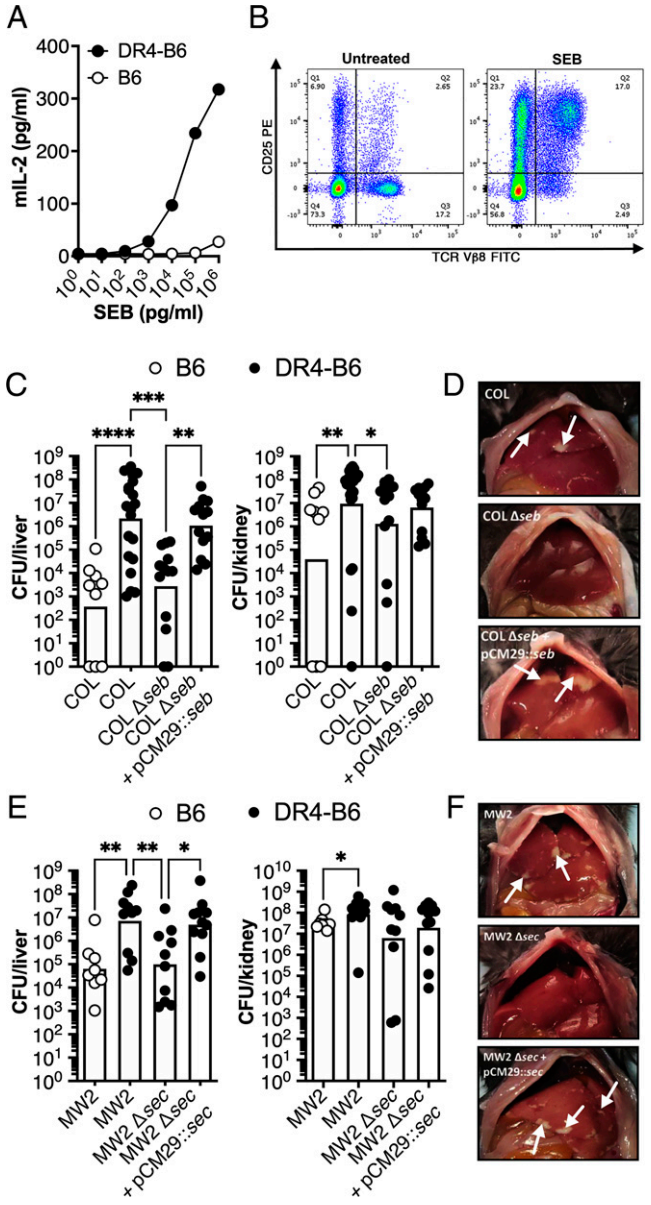

Fig. 1. SAgs SEB and SEC promote pathogenesis of *S. aureus* bacteremia in transgenic HLA-DR4 B6 animals. (*A*) IL-2 production of isolated splenocytes from conventional B6 (open dots) and transgenic DR4-B6 (solid dots) mice following stimulation with a titration of SEB protein. Data shown are from a representative experiment. (*B*) Activation of $V\beta8^+$ T cells in DR4-B6 mice stimulated by SEB compared to an untreated control as determined by CD25 expression (quarter values represent total cell population). (*C*–*F*) B6 and DR4-B6 animals were inoculated i.v. with 5×10^6 CFUs and then killed at 96 hpi for *S. aureus* COL (*C* and *D*) and 72 hpi for *S. aureus* MW2 (*E* and *F*). Liver and kidney bacterial burden (*C* and *E*) was assessed in conventional B6 mice (open dots) or in transgenic DR4-B6 mice (solid dots). Each dot represents an individual mouse, and the bar indicates the geometric mean. Significant differences were determined using the Kruskal–Wallis test with the uncorrected Dunn's test for multiple comparisons (*$P < 0.05$, **$P < 0.01$, ***$P < 0.001$, ****$P < 0.0001$). Representative livers from the infected mice from *S. aureus* COL and mutants (*D*) and *S. aureus* MW2 and mutants (*F*) with white arrows indicate the presence of liver lesions.

Depletion of $CD4^+$ T Cells Results in Reduced Bacterial Burden in the Liver of *S. aureus*–Infected DR4-B6 Mice. It has been well established that SAgs can target and activate different T cell subsets that express the appropriate TCR Vβ (10). For efficient nasopharyngeal infection, *Streptococcus pyogenes* required the expression of the SAg streptococcal pyrogenic exotoxin A (SpeA) (22), and depletion of T cells resulted in a markedly reduced bacterial burden, which phenocopied the deletion of

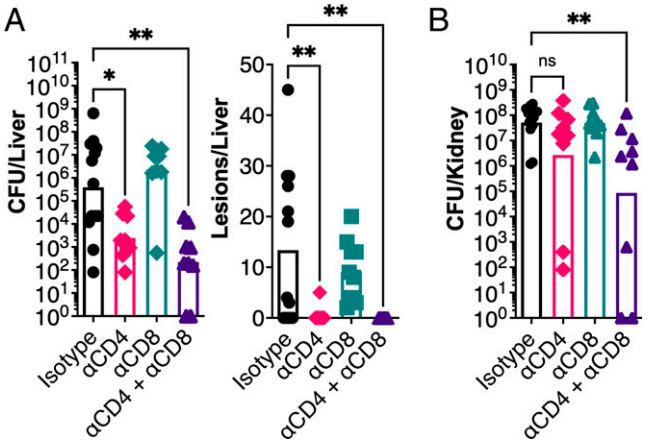

Fig. 2. CD4$^+$ T cells promote bacterial burden during *S. aureus* bloodstream infection. In vivo T cell depletion in DR4-B6 mice was performed with monoclonal antibodies to deplete CD4$^+$ (clone GK1.5) and/or CD8$^+$ (clone YTS169.4) cells prior to i.v. infection with *S. aureus* COL. (*A* and *B*) In vivo liver bacterial burdens and pathology (*A*) and kidney bacterial burdens (*B*) were assessed 96 hpi. Each data point represents an individual mouse, and the bar indicates the geometric mean for CFUs/organ and the median for lesions/organ. Significant differences were determined using the Kruskal–Wallis test with the uncorrected Dunn's test for multiple comparisons (*$P < 0.05$, **$P < 0.01$). ns, not significant.

the *speA* gene (23). In the current study, we used this T cell depletion strategy and applied it to our model of *S. aureus* bacteremia. We found that when CD4$^+$ T cells were depleted, bacterial burden in the liver was significantly reduced, with a near-complete reduction of visible lesions, while depletion of CD8$^+$ T cells had no impact (Fig. 2*A*). To reduce bacterial burden in the kidneys, depletion of CD4$^+$ T cells was not sufficient and required the combined depletion of CD4$^+$ and CD8$^+$ T cells to observe a phenotype, suggesting a role for CD8$^+$ cells in this organ (Fig. 2*B*). To determine if this effect was limited to conventional CD4$^+$ T cells, we also depleted natural killer (NK) and invariant NKT cells using an anti-NK1.1 targeting antibody, according to a previously established protocol (24). In this case, there was no impact on bacterial burden or animal morbidity, indicating these cells likely do not play a role in this infection model (*SI Appendix*, Fig. S2). Altogether, these data indicate that bacterial burden in the liver during *S. aureus* bacteremia is promoted by the activity of conventional CD4$^+$ T cells, likely due to activation by SEB.

Blocking of IFN-γ Activity during Systemic *S. aureus* Infection Results in Reduced Disease Severity and Bacterial Burden. Previous analyses have demonstrated that CD4$^+$ T cells can be targeted by staphylococcal SAgs to result in the release of numerous cytokines including the key cytokines IFN-γ (also known as type II interferon), interleukin-10 (IL-10), and interleukin-17A (IL-17A) (10). These cytokines have antagonistic activity toward each other (25, 26) and, in the case of IL-17A and IFN-γ, have been shown to contribute to SEB-mediated morbidity during toxemia models in HLA-transgenic mice (27, 28). Together, this suggests that these key cytokines may contribute to SAg-mediated pathogenesis. To test this hypothesis, we used antibody depletion to block cytokine activity during bloodstream infection by both *S. aureus* COL and MW2 (Fig. 3*A*). We found that blocking IFN-γ resulted in a significant reduction in bacterial liver burden and liver pathology that phenocopied the deletion of *seb* or *sec* in *S. aureus* COL and MW2, respectively (Fig. 3 *B*, *D*, *E*, and *G*). However, depletion of either IL-10 or IL-17A had limited impact on the liver burden, suggesting that these cytokines do not promote bacterial burden in this model. Depletion of IFN-γ also resulted in lower bacterial burden in the kidneys, suggesting that the blocking of this cytokine reduced the overall severity of the infection (Fig. 3 *C* and *F*). It was also noted that bacterial burden in the kidneys increased once IL-17A was depleted but only for *S. aureus* COL. This suggests that IL-17A contributes to protection against kidney damage during bloodstream infection by *S. aureus* in the HLA-transgenic mouse model. Overall, these data indicate that, of the three cytokines tested, only IFN-γ promoted *S. aureus* burden during a bloodstream infection.

SAgs Drive Pathogenic Production of IFN-γ during *S. aureus* Bloodstream Infection. Several approaches were taken to determine if the promotion of bacterial burden by IFN-γ was mediated by the SAg toxins. First, we performed cytokine analysis on liver homogenates and serum from animals infected with the wild type or the SAg-deletion mutants at 24 h postinfection (hpi). Compared to wild-type *S. aureus* COL–infected mice, IFN-γ levels were ∼10-fold lower in livers from animals infected with *S. aureus* COL Δ*seb* (Fig. 4*A*). There was also a clear trend for more IFN-γ in the serum for animals that were infected with the wild type, although this did not reach statistical significance (Fig. 4*A*).

Following from the cytokine analysis, we modified our infection model to characterize IFN-γ depletion under circumstances in which the SEB SAg from *S. aureus* COL was either absent or unable to function. In the SAg-insensitive B6 background, bacterial recovery from infected mice was comparatively low regardless of IFN-γ–depletion treatment, suggesting that this phenotype could only be observed in a SAg-sensitive environment (Fig. 4*B*). Indeed, when we repeated the IFN-γ depletion in the DR4-B6 background and included the COL Δ*seb* construct, bacteria recovered from organs of the isotype or IFN-γ–depleted groups were similarly low, whereas wild-type infections treated with the isotype control antibody produced visible liver lesions and higher bacterial counts in both the liver and kidneys (Fig. 4*B*). These data demonstrate that a functioning *seb* gene is required to promote pathogenic IFN-γ activity.

Finally, to establish the link between SEB and IFN-γ, we aimed to determine if the addition of exogeneous IFN-γ could functionally complement the deletion of *seb* in *S. aureus* COL. In this experiment, animals were administered two 20-μg treatments of recombinant IFN-γ 2 h prior to infection and 1 h after. Treatment with exogenous IFN-γ resulted in a ∼2-log increase in bacterial burden in the liver when compared to the vehicle control (Fig. 4*C*). Curiously, very few lesions formed on the surface of the liver with this approach, suggesting that sustained SAg/IFN-γ activity is required for pathology to become evident (Fig. 4*C*). This demonstrates that the stimulation of pathogenic IFN-γ is a key function of SEB during bloodstream infection and, taken together with the previous data, suggests that a functional SAg must be present to elicit pathogenic production of IFN-γ.

IFN-γ Promotes Early Bacterial Survival during *S. aureus* Infection. With it established that SAgs could drive the production of pathogenic levels of IFN-γ, we next wanted to determine when IFN-γ had the most impact during the disease course. Therefore, we determined bacterial burden at shorter time points (i.e., 2 to 36 hpi) in animals treated with αIFN-γ antibodies (monoclonal antibodies specific for IFN-γ) or an isotype control antibody (Fig. 5*A*). From these experiments, we determined that much of the infectious dose became trapped within the liver following tail-vein injection with ∼2×10^6 colony-forming units (CFU) at 2 hpi (∼40% of the dose), and this was followed by rapid clearance between 2 and 8 hpi in both groups. At 12 hpi, the rate of bacterial clearance was reduced in the αIFN-γ–treated animals but continued steadily with almost complete clearance of the bacteria by 96 hpi. Conversely, after 24 hpi in the livers of isotype

MICROBIOLOGY

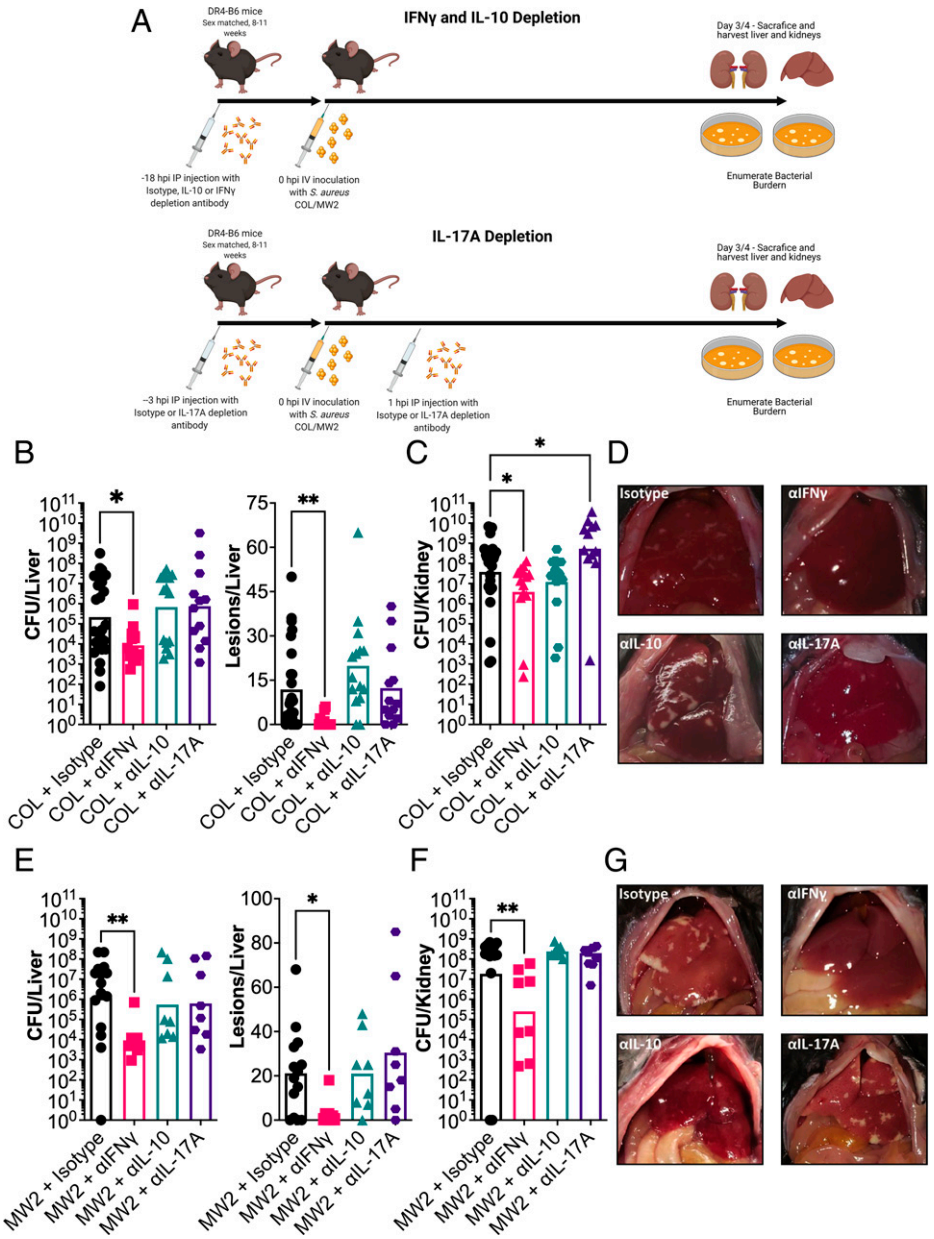

Fig. 3. IFN-γ promotes liver abscess formation and bacterial burden during *S. aureus* bacteremia in DR4-B6 mice. (*A*) Schematic outlining in vivo cytokine depletion with monoclonal antibodies prior to i.v. infection of DR4-B6 mice. (*B*, *C*, *E*, and *F*) Bacterial burden and abscess formation in liver (*B* and *E*) and kidneys (*C* and *F*) at 96 hpi for *S. aureus* COL (*B* and *C*) or 72 hpi for *S. aureus* MW2 (*E* and *F*). Each dot represents an individual mouse, and the bar represents the geometric mean for CFUs/organ and the median for lesions/organ. Significant differences were determined using the Kruskal–Wallis test with the uncorrected Dunn's test for multiple comparisons (*$P < 0.05$, **$P < 0.01$). (*D* and *G*) Representative livers are shown from the cytokine-treated mice from *S. aureus* COL (*D*) and *S. aureus* MW2 (*G*).

antibody–treated mice, bacterial burdens rapidly expanded, reaching a level ∼3-logs higher by 96 hpi (Fig. 5*A*). We performed a repeat of this analysis with daily time points and were able to confirm the trajectories that were observed in the shorter time course (*SI Appendix*, Fig. S3). Together, these data indicate that IFN-γ produced during infection by wild-type *S. aureus* is contributing to the ability of the bacteria to avoid clearance by the immune system in the liver during the early stages of bloodstream infection.

Proinflammatory Signaling Is Delayed and Less Intense When IFN-γ Is Blocked during Sepsis. IFN-γ is a pleiotropic cytokine of the immune system, and its depletion during infection could impact numerous downstream signaling pathways during the response to *S. aureus* bloodstream infection. In isotype antibody–treated mice, the highest level of IFN-γ was observed in the liver between 12 and 24 hpi, in excess of 500 pg/mL (Fig. 5*B*). Additionally, we confirmed that αIFN-γ antibodies were able to reduce IFN-γ concentration during infection up to 36 hpi (Fig. 5*B*). We also analyzed serum samples for aspartate aminotransferase (AST) levels as a proxy for liver damage. These data indicate that there was limited change in liver damage during infection irrespective of IFN-γ levels; however, there did appear to be a faster drop in AST levels in the IFN-γ–depleted groups in the later time points (Fig. 5*C*), congruent with the reduced bacterial burden (Fig. 5*A*).

To gain a broader understanding of the cytokine and chemokine dynamics, liver homogenates were analyzed by multiplex

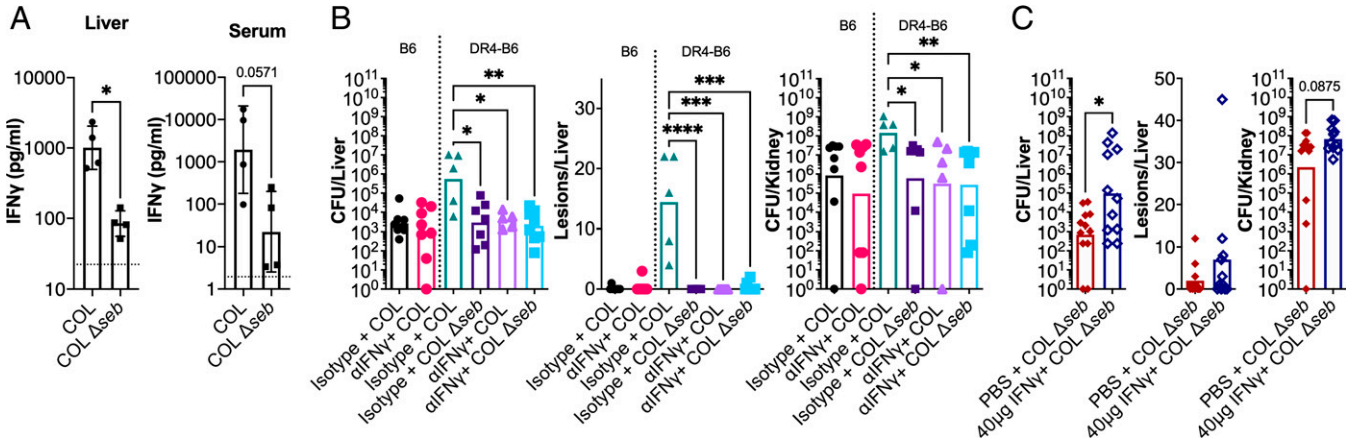

Fig. 4. SAgs promote pathogenic production of IFN-γ that supports bacterial burden. (*A*) DR4-B6 mice were inoculated i.v. with wild-type *S. aureus* COL or the COL Δ*seb* deletion strain. At 24 hpi, animals were killed, livers and blood were harvested, and material was prepared for IFN-γ analysis. Each dot represents an individual mouse, the bar indicates the geometric mean, and error bars indicate the SD. The dotted line indicates the levels detected in an uninfected animal. (*B*) B6 and DR4-B6 mice were treated 18 h prior to infection with 250 μg isotype control or αIFN-γ antibody administered by i.p. injection and animals were infected i.v. with wild-type *S. aureus* COL or COL Δ*seb*. (*C*) DR4-B6 animals were treated with 20 μg (40 μg total) recombinant murine IFN-γ or vehicle control (100 μL PBS) i.p. 2 h before and 1 h after i.v. infection with *S. aureus* COL Δ*seb*. In both experiments (*B* and *C*), in vivo bacterial burden was assessed after 96 h in liver and kidneys and an assessment of gross pathological liver lesions was also performed. Each dot represents an individual mouse, and the bar indicates the geometric mean for CFUs/organ and the median for lesions/organ. Significant differences were determined using the Mann–Whitney *U* test or Kruskal–Wallis test with the uncorrected Dunn's test for multiple comparisons (*$P < 0.05$, **$P < 0.01$, ***$P < 0.001$, ****$P < 0.0001$).

cytokine array over the course of the experiment. This demonstrated that in earlier time points (2 to 12 hpi), many signaling molecules associated with inflammation were up-regulated during infections in which IFN-γ was produced at high levels (Fig. 5*D*). Strikingly, between 24 and 36 hpi, many cytokines and chemokines became reduced relative to the group treated with αIFN-γ antibodies, which directly correlated with the expansion of *S. aureus* (Fig. 5*A*) and was subsequently reversed again by 96 hpi (Fig. 5*D*). This suggests that an inflammatory environment favorable to bacterial proliferation is sustained for a longer period during infections in which IFN-γ production is relatively high. Altogether, we infer that pathogenic production of IFN-γ results in the rapid production of a proinflammatory environment in the liver that contributes to *S. aureus* survival during bloodstream infection.

Macrophage Activity in the Liver Is Subverted by SAg-Elicited IFN-γ Production. Immune cells, such as macrophages and neutrophils, are critical for clearance of *S. aureus* during infection (29, 30). The cytokine and chemokine analysis indicated that wild-type *S. aureus* infection in HLA-DR4 mice drives an IFN-γ–dependent proinflammatory signaling cascade in the livers of animals (Fig. 5*D*). To determine if this response had any impact on the phagocytic cell populations in the liver, we first phenotyped immune cells isolated from this organ using flow cytometry at 24 and 96 hpi infection with *S. aureus* COL (*SI Appendix*, Fig. S4 provides the gating strategy). We found few differences between the IFN-γ–depleted or control mice in terms of the resident macrophages (Kupffer cells) (Fig. 6*A*). For both monocytes and neutrophils, there were trends toward a higher percentage of these cells at 24 hpi in the isotype antibody–treated group; however, neither reached significance (Fig. 6*A*). For neutrophils, this had subsided to a similar level in both groups by 96 hpi, whereas monocytes had decreased in both groups by 96 hpi, but there were significantly fewer in the IFN-γ–depleted group at this time. We did detect significantly higher inflammatory macrophages in the IFN-γ–depleted mice at 24 hpi, although these were equivalent by 96 hpi (Fig. 6*A*).

The infection kinetics (Fig. 5*A*) and flow cytometry (Fig. 6*A*) analyses suggest that the presence of high levels of IFN-γ could impact the activity, recruitment, or differentiation of phagocytes, most likely inflammatory macrophages. To determine if these cells are the target of pathogenic IFN-γ production, we depleted macrophages in mice using clodronate containing liposomes (Clodrosome) and then performed *S. aureus* COL bloodstream infections with or without IFN-γ–blocking antibodies (Fig. 6*B*). Macrophage depletion had a negative impact on animal welfare, so end points were brought forward from 96 hpi to 72 hpi and bacterial burden was determined in both the kidneys and the liver. In the liver, we again observed, at 24 hpi in animals treated with the control liposomes, that IFN-γ depletion resulted in a higher bacterial burden (Fig. 6*C*). However, when we compared macrophage-depleted animals, the phenotype observed between the IFN-γ depletion and isotype antibody groups was abolished, indicating that macrophages are likely required for the IFN-γ–dependent phenotype. We also observed an increase in bacterial burden when macrophages were depleted, compared to animals treated with control liposomes and isotype antibody (Fig. 6*C*), indicating that these cells were important to restrict bacterial growth in the liver at this time point. In the kidneys, there was evidence that the depletion of macrophages likely resulted in greater bacterial "seeding" to this organ, although there was no difference due to IFN-γ depletion (Fig. 6*C*). The data from the 72-hpi time point confirmed the observation that macrophages were necessary for the IFN-γ phenotype, as again, we were able to observe a clear IFN-γ phenotype in both the kidneys and liver, yet this phenotype was mitigated by macrophage depletion (Fig. 6*C*). Together, these data demonstrate that the promotion of *S. aureus* burden by IFN-γ during bloodstream infection is mediated by macrophages.

High Levels of IFN-γ Allow for Increased Intracellular Replication of *S. aureus* inside Human Macrophages. To determine if pathogenic IFN-γ had any impact in the human system, white blood cells from healthy human donors were analyzed for their responses to SAgs and IFN-γ. First, we wanted to confirm that SAgs can elicit IFN-γ from T cells through the engagement of the TCR. To do this, we compared IFN-γ production elicited by recombinant SEB protein compared to the site-directed mutant SEB-N23A. This mutant features a mutation within the TCR binding pocket resulting in a much lower ability to engage the TCR of

MICROBIOLOGY

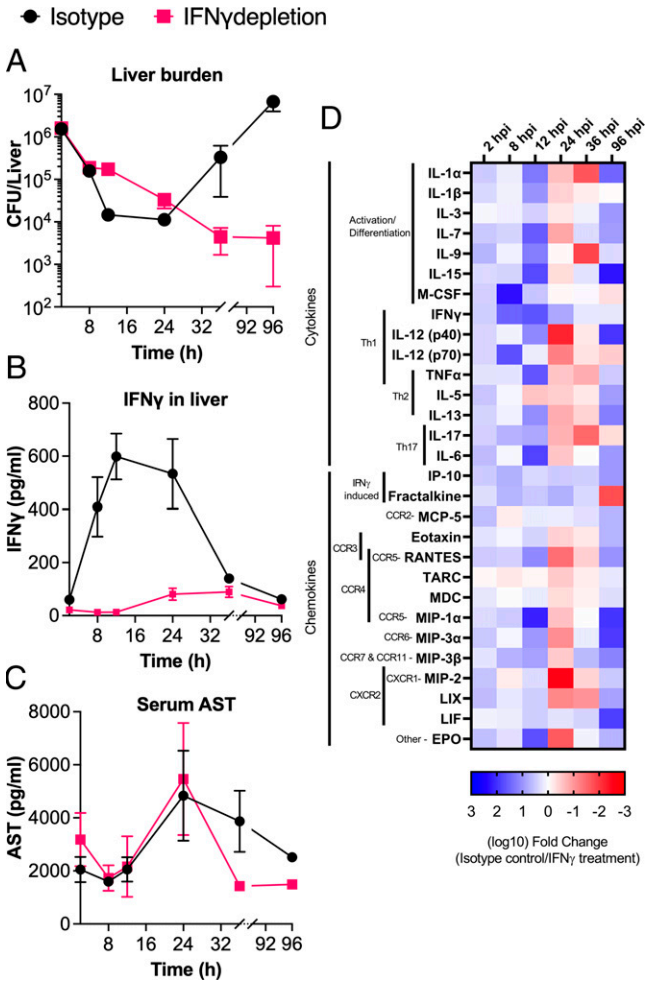

Fig. 5. SAg-induced IFN-γ promotes a proinflammatory environment that allows *S. aureus* to impede clearance during bloodstream infection. DR4-B6 mice were treated with isotype antibody or IFN-γ–depleting antibodies 18 h prior to infection with *S. aureus* COL. Following infection, three to four animals were killed from each group at the six time points shown, and liver and blood were harvested from each animal. (*A*) Bacterial burden was determined at each time point and is shown as mean CFU/liver ± SEM. (*B*) Liver homogenate was analyzed by multiplex cytokine array, and mean IFN-γ (pg/mL) ± SEM at each time point were determined for each time point. (*C*) Serum was analyzed by ELISA to determine the concentration of AST. Data shown are mean AST (pg/mL) ± SEM. (*D*) Multiplex cytokine/chemokine array analysis was conducted on liver homogenate recovered from each animal killed during the time course. Data shown represent the $\log_{10}$ fold change for each cytokine between isotype antibody– and IFN-γ–depleted groups that displayed significant differences by Student's *t* test. Prior to comparison, data were normalized to an antibody-treated, uninfected animal killed at the same time point as their comparator. Blue color (i.e., positive values) indicates that more cytokine/chemokine is produced in the isotype antibody infection, and red color (i.e., negative values) indicates that more cytokine/chemokine is produced in the IFN-γ–depleted infection. Broad classification for each cytokine is indicated as well as potential binding partners for chemokines.

its target cells (31). As expected, SEB-N23A elicited significantly lower IFN-γ from human peripheral blood mononuclear cells (PBMCs) compared with wild-type SEB (Fig. 7*A*). This confirmed that to elicit IFN-γ from human PBMCs, SEB must engage and activate the T cell through binding the TCR.

Next, we wanted to establish that our experimental strains (i.e., COL and MW2) could elicit IFN-γ production from human PBMCs. We stimulated human PBMCs with a titration of wild-type bacterial supernatants grown for 8 h in brain heart infusion (BHI) broth and included supernatants from the respective SAg-deletion and complemented strains. The data clearly indicated that both SEB and SEC, produced from COL and MW2, respectively, could drive IFN-γ production in human PBMCs (Fig. 7 *B* and *C*). The deletion of *seb* in COL eliminated the production of IFN-γ, while there was a significant decline in the potency of MW2 Δ*sec*. The remaining IFN-γ production was still easily detectable at lower MW2 Δ*sec* supernatant dilutions, suggesting that other SAgs encoded by MW2 (i.e., *sea*, *selh*, *selk*, *sell*, *selq*, *selw*, and *selx*) are also able to elicit the production of this cytokine.

As the murine model indicated that macrophages are likely the major target of SAg-induced IFN-γ, we infected both murine and human macrophages with *S. aureus* and dosed these cells with varying concentrations of recombinant IFN-γ (Fig. 7 *D* and *G*). With murine macrophages, we initially tested bone marrow–derived macrophages (BMDMs) from DR4-B6 animals but observed limited *S. aureus* replication in these cells (*SI Appendix*, Fig. S5). Therefore, we moved this analysis into RAW 264.7 cells (a murine macrophage cell line), which have been shown to be permissive to *S. aureus* replication (32). For both *S. aureus* COL and MW2, we saw an overall increase in intracellular bacterial replication when murine macrophages were dosed with high levels of IFN-γ, although this was most evident with *S. aureus* COL, which exhibited a ∼2-log increase as IFN-γ levels increased (Fig. 7 *E* and *F*). However, in human monocyte-derived macrophages, the IFN-γ phenotype was most evident with MW2, as this strain seemed to have an improved ability at replicating inside human macrophages and also exhibited a ∼2-log increase at the highest IFN-γ concentrations (Fig. 7 *H* and *I*). Notably, the high concentrations of IFN-γ did not impact macrophage viability, and the bacteria were not simply overgrowing dead macrophages (*SI Appendix*, Fig. S6). Together, these data indicate that SAg-induced, IFN-γ–mediated subversion of macrophages can occur in both the murine and human system and that this mechanism appears to impair the ability of macrophages to kill intracellular *S. aureus*.

Discussion

Bloodstream infections caused by *S. aureus* represent a significant challenge in the clinic, and SAgs have been demonstrated to be important in this disease (reviewed in refs. 2 and 11). However, it has remained unclear how SAgs promote *S. aureus* persistence during infection and, specifically, how these toxins manipulate the immune response (10). The weak activity of SAgs in murine models has been a serious challenge for our understanding as to how these toxins promote bacterial burden during infection. While rabbits are more sensitive to SAg activity and may be more physiologically appropriate, challenges include both cost and the availability of advanced immunological tools (33). Using the HLA-transgenic mouse model, we established that IFN-γ can be promoted to pathogenic levels by the SAgs SEB and SEC, showing how a key cytokine produced in response to SAg-mediated T cell activation dramatically promotes bacterial burden during a systemic infection. This research adds to a growing body of literature that explains how these toxins function to subvert different components of the immune system and challenges the waning dogma that these proteins are produced by the bacterium simply as an "immunological smoke screen" (reviewed in ref. 10).

The pathogenic potential of IFN-γ in *S. aureus* disease has been alluded to in other studies. Firstly, a model of wound infection indicated that *S. aureus* capsular polysaccharide was shown to elicit IFN-γ, which led to an increased recruitment of neutrophils (34). The authors postulated that higher neutrophil recruitment increased pathogenesis, as *S. aureus* was able to avoid neutrophil killing and survive intracellularly (34). Our

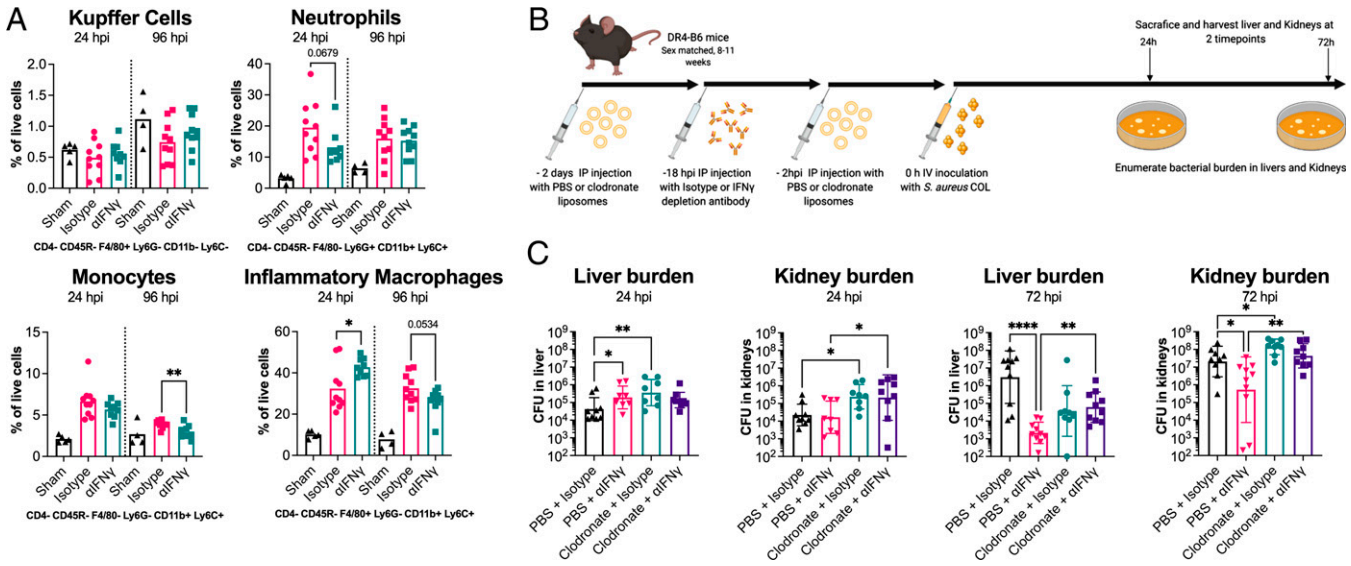

Fig. 6. Liver macrophages are the target of pathogenic IFN-γ production. (*A*) Flow cytometry–based phenotyping of immune cells isolated from livers of mice infected with *S. aureus* strain COL at 24 and 96 hpi. Control animals (sham) were treated with HBSS only. Cells were defined based on the staining profile listed below each graph and normalized to the percentage of live cells. Isotype antibody and αIFN-γ treatments were compared; each dot represents an individual mouse, and the bar indicates the mean. Significant differences were determined using an unpaired Welch's *t* test (*$P < 0.05$, **$P < 0.01$). (*B*) Schematic outlining Clodronate liposome-based depletion of macrophages along with IFN-γ depletion used prior to i.v. infection of mice with *S. aureus* COL. (*C*) Bacterial burden in liver and kidneys at 24 and 72 hpi is shown. Each dot represents an individual mouse, and the bar represents the geometric mean for CFUs/organ. Significant differences were determined using the Kruskal–Wallis test with the uncorrected Dunn's test for multiple comparisons (*$P < 0.05$, **$P < 0.01$, ****$P < 0.0001$).

cytokine/chemokine data are consistent with these findings (Fig. 5*D*), and while neutrophils were trending toward lower recruitment in the IFN-γ–depleted group at 24 hpi (Fig. 6*A*), it appeared to be monocytes and inflammatory macrophages, rather than neutrophils in the isotype antibody–treated group, that were recruited to the liver by 96 hpi (Fig. 6*A*). This variation in immune-cell recruitment could promote a niche for the bacteria to reside within in the liver. Furthermore, our data also indicated IFN-γ drove an increased production of the chemokine fractalkine (CX3CL1), which has been suggested to be able to skew liver macrophages toward a more suppressive state (35). Added to this, high levels of IFN-γ were able to induce apoptosis and affect the life cycle of hepatocytes, which can contribute to sustained inflammation in this organ (36). Together, these observations, both in this study and others, suggest that SAgs, through forcing the overproduction of IFN-γ, can modulate the liver environment to create a niche that is favorable for *S. aureus* survival.

The liver is an important organ during bacteremia, as circulating pathogens are frequently filtered and trapped by resident Kupffer cells (37). In addition, there have been several reports that demonstrate that *S. aureus* has evolved strategies to prevent this from occurring, including direct resistance to phagocytic killing by macrophages or through the release of Hla that can aggregate platelets to create ischemic areas in the liver and promote further bacterial growth (37, 38). It is important for the bacteria to establish in the liver, as bacteria surviving here can eventually seed other organs such as the kidneys (37, 39).

Given the pleotropic nature of IFN-γ, it is not surprising that several mechanisms may be at play in the liver to promote the growth of *S. aureus*. In addition to the other potential mechanisms of action defined in other studies, we have evidence that suggests a pathway in which macrophages are a clear target of pathogenic levels of IFN-γ. It has been suggested previously that macrophages may be influenced by the immune dysregulation caused by SAgs, as there were reports during the early stages of the menstrual toxic shock syndrome (mTSS) epidemic that found that macrophages from affected patients exhibited erythrophagocytosis (40). However, here we demonstrate that macrophage activity has been shown to be affected by high concentration of IFN-γ to support intracellular replication of *S. aureus*.

Our findings could also appear to be somewhat contradictory to several other studies that clearly demonstrate that IFN-γ contributes to the clearance of *S. aureus* during bloodstream infection (41, 42). Furthermore, the activity of memory $CD4^+$ T cells supports the clearance of *S. aureus* by producing this cytokine along with other signals to coordinate this response (41). These studies were conducted in conventional mouse strains that are less vulnerable to the activity of staphylococcal SAgs and are more likely to represent what would occur in an immunocompetent individual with preexisting SAg-neutralizing antibodies. Indeed, this divergence is revealed by Brown et al., where mice previously exposed to *S. aureus* demonstrated an IFN-γ peak almost immediately after infection and subsequently dropped rapidly, whereas in mice that were not preexposed to *S. aureus,* IFN-γ was barely detected (41). This is contrary to what we have observed in SAg-mediated disease, as IFN-γ peaked later (24 hpi) and stayed high for much of the infection course. Altogether, this suggests that IFN-γ has a dual role during infection. Primarily, it is protective against *S. aureus*, but if manipulated to high and sustained levels, IFN-γ can act as a mediator to promote pathogenesis.

The implications of pathogenic IFN-γ production in human health are significant. As discussed, *S. aureus* is one of the most common causes of bloodstream infection, with disease often leading to life-threatening sepsis (2). Indeed, sepsis is a very serious concern in the clinic, contributing to nearly 20% of global annual deaths (43). One of the major challenges to treating sepsis is that without early intervention, this disease can rapidly move from a microbiologically mediated condition to an immunologically driven sequela, often resulting in antibiotic treatment being ineffective (3). The pathophysiology of sepsis has also proven to be highly complex, with many factors,

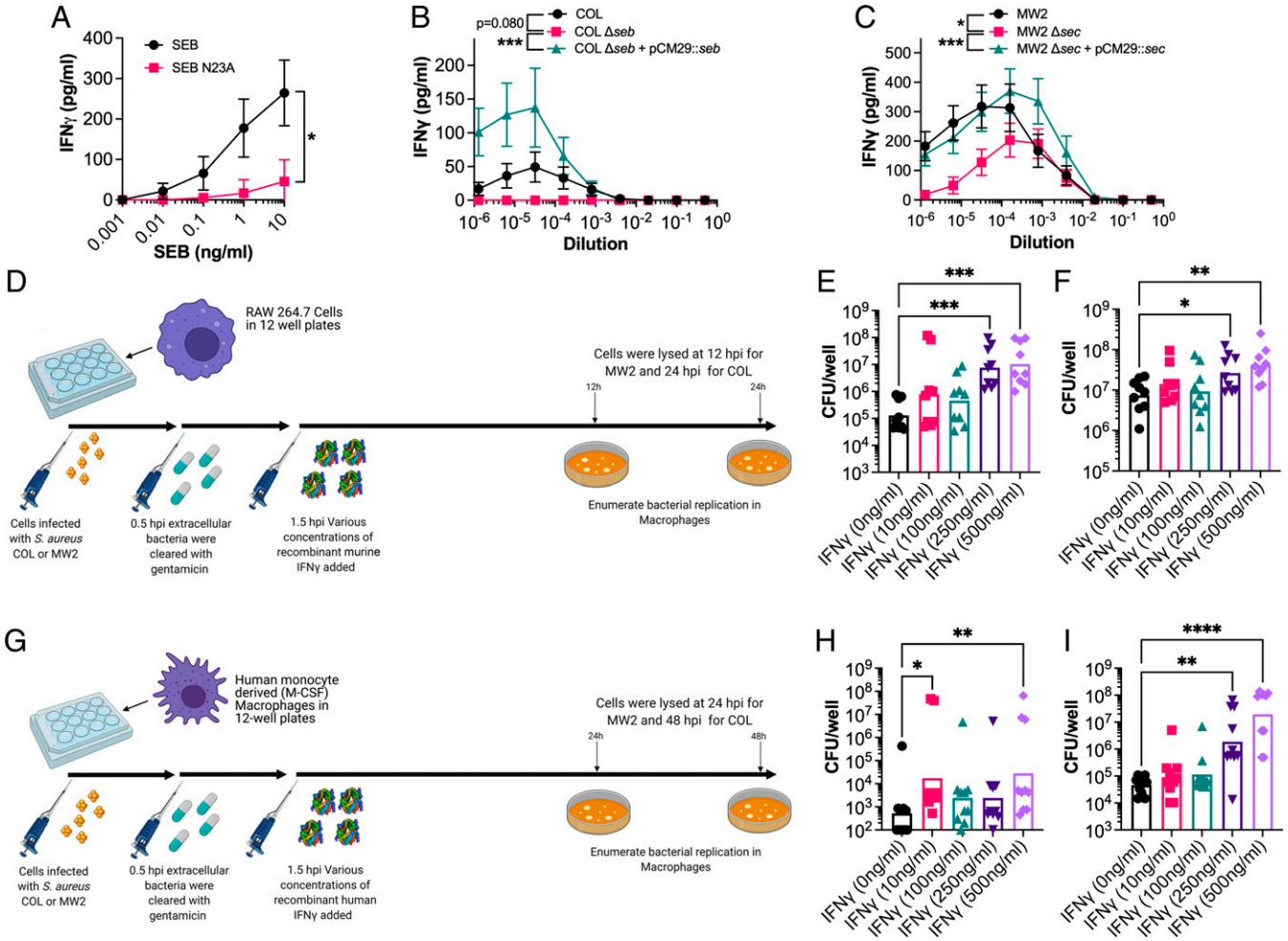

Fig. 7. SEB and SEC elicit IFN-γ from human cells, and excessive concentration can promote increased extracellular replication of *S. aureus* in macrophages. (*A*) IFN-γ production by PBMCs from human blood following stimulation with a titration of SEB or the SEB-N23A proteins. (*B* and *C*) IFN-γ production by PBMCs from human blood following stimulation with a titration of supernatant from *S. aureus* COL (*B*) or MW2 (*C*) strains as indicated. Supernatants were taken from cultures grown for 8 h in BHI prior to use in these assays. Data shown (*A*–*C*) are mean ± SEM from eight donors. Significant differences were determined from the area under each curve using a paired Friedman test for multiple comparisons (*$P < 0.05$, ***$P < 0.001$). (*D*) Schematic outlining the procedure for intracellular *S. aureus* replication in RAW 264.7 murine macrophages after dosing with recombinant murine IFN-γ. (*E* and *F*) *S. aureus* recovered from RAW 264.7 cells after incubation at 24 h for strain COL (*E*) and 12 h for strain MW2 (*F*) with varying concentrations of recombinant IFN-γ. Each dot represents an individual experiment, and the bar represents the geometric mean for CFUs/well. (*G*) Schematic outlining the procedure for intracellular *S. aureus* replication in monocyte-derived human macrophages after dosing with recombinant human IFN-γ. (*H* and *I*) *S. aureus* recovered from human macrophages after incubation at 48 h for strain COL (*H*) and 24 h for strain MW2 (*I*) with varying concentrations of recombinant IFN-γ. Each dot represents macrophages from an individual human donor, and the bar represents the geometric mean for CFUs/well. Significant differences between 0 ng/mL of IFN-γ and other concentrations were determined using the Kruskal–Wallis test with the uncorrected Dunn's test for multiple comparisons (*$P < 0.05$, **$P < 0.01$, ****$P < 0.0001$).

including the invading pathogen, contributing to outcome. Death as an outcome of sepsis can occur both through acute inflammatory processes that lead to multiorgan failure as well as chronic immunosuppressive activity (44). In both cases, IFN-γ can contribute to these outcomes as a key promoter of the proinflammatory response or due to its absence leading to the dominance of immunosuppressive pathways (45, 46). Indeed, several studies have demonstrated that once a patient enters the immunosuppressive state of sepsis, therapy with IFN-γ may actually improve outcomes; however, the opposite may be true if administered too early (47, 48).

There is also evidence to suggest that this mechanism may be at play in the context of *S. aureus* vaccines and could be an important consideration for vaccine design. Karauzum et al. found that whole-cell vaccines in mice promoted disease and bacterial survival through the activity of a heavily skewed Th1 immune response (49). It appeared in this bloodstream infection model that disease was promoted by the vaccines and that this was mediated by excessive production of IFN-γ. It was also suggested that this study had significant parallels with the failure of a clinical trial using the IsdB subunit vaccine, which was intended to protect against bacteremia but instead had to be terminated early as it worsened patient outcome (49, 50). Altogether, this would suggest that *S. aureus* has evolved to take advantage of a human immune system whose responses have been skewed by the activity of IFN-γ and, further, evolved a family of toxins capable of driving this skewing itself.

In conclusion, we report the discovery that *S. aureus* SAgs can drive the production of IFN-γ during bloodstream infection to promote disease. Our analyses suggest that the pathogenic production of IFN-γ subverts macrophage activity, allowing the bacterium to persist within the liver and leading to increased morbidity. Furthermore, we were able to establish that this mechanism has implications for human health, as high levels of

IFN-γ can promote bacterial intracellular replication in human macrophages. Altogether, this moves forward our understanding of the immunological factors at play during *S. aureus*–meditated sepsis in the context of pathogen-driven inflammation and may help inform the appropriate design of treatments and vaccines targeting *S. aureus* disease.

Materials and Methods

Human Ethics Statement. Human venous blood was taken from healthy volunteer donors in accordance with human subject protocol 110859. The full study protocol was approved by the London Health Sciences Centre Research Ethics Board (University of Western Ontario, London, ON, Canada). Volunteers were recruited by a passive advertising campaign within the Department of Microbiology and Immunology at the University of Western Ontario, and following an outline of the risks, written informed consent was given by each volunteer before each sample was taken. Following sampling, blood was fully anonymized and no information regarding the identity of the donor, including sex and age, was retained.

Mice. Male and female (8- to 11-wk-old) HLA-DR4-IE (DRB1*0401) humanized transgenic mice lacking endogenous mouse MHC-II on a C57BL/6 (B6) background (here referred to as DR4-B6 mice) (38), or B6 mice, were used for all in vivo infection experiments. DR4-B6 animals were bred on site at the University of Western Ontario, and B6 mice were purchased from the Jackson Laboratory (Stock No. 000664). Animals for experiments were housed in single-sex cages, which did not exceed four in number. During all breeding and experiments, mice were provided food and water ad libitum and appropriate enrichment was provided in all cages. All animal experiments were in accordance with the Canadian Council on Animal Care Guide to the Care and Use of Experimental Animals, and the animal protocol was approved by the Animal Use Subcommittee at the University of Western Ontario.

Bacterial Strains, Media, and Growth Conditions. *S. aureus* strains listed in *SI Appendix*, Table S1 were grown aerobically at 37 °C in tryptic soy broth (TSB) (Difco) or BHI broth with shaking (250 rpm) supplemented with appropriate antibiotics. For solid-phase cultures, tryptic soy agar (TSA) was used (TSB containing 1.5% wt/vol agar) supplemented with the appropriate antibiotics. *Escherichia coli* strains were used as cloning hosts and were grown in Luria–Bertani (LB) broth (Difco) or LB agar supplemented with appropriate antibiotics at 37 °C with shaking (250 rpm). Growth curve analysis was performed using a Biotek Synergy H4 multimode plate reader.

Construction of MW2 Δ*sec* Mutant. Markerless deletion of *sec* in MW2 was performed using the pKOR1 allelic replacement system (51). The *sec* knockout was created as described previously (51), and candidate constructs were screened by PCR using primers SEC-screen-For and SEC-screen-Rev (*SI Appendix*, Table S2). See *SI Appendix, SI Materials and Methods* for more details.

Construction of pCM29::*seb* and pCM29::*sec* Complementation Plasmids. SEB and SEC complementation plasmids for *S. aureus* SAg null mutants were created as previously described, with modifications (17). See *SI Appendix, SI Materials and Methods* for more details. After this step, ligations were transformed into *E. coli* SA30B (52) for appropriate methylation before transformation of sequence positive constructs into electrocompetent *S. aureus* using a protocol previously described (53).

Protein Expression and Purification. Recombinant SEB was generated as described previously (54). Briefly, SEB was expressed with a His-tag in BL21 (DE3) *E. coli* and purified by nickel column chromatography. An attenuated mutant of SEB that has impaired binding to TCR was also purified. The mutant SEB carries an N→A point mutation at position 23 and is referred to as SEB_{N23A} (31, 55). The experimental use of SEB was approved by the University of Western Ontario Biosafety Committee (application no. BIO-UWO-0155).

Murine Splenocyte Analysis. The ability of murine cells to respond to SEB was determined using IL-2 production. Mouse spleens were removed and broken into a single-cell suspension, followed by red blood cell lysis in ammonium–chloride–potassium (ACK) buffer. The remaining cells were suspended in complete RPMI (cRPMI), containing RPMI (Invitrogen Life Technologies) supplemented with 10% fetal bovine serum (FBS) (Wisent Inc.), 100 μg/mL streptomycin, 100 U/mL penicillin (Gibco), 2 mM l-glutamine (Gibco), 1 mM sodium pyruvate (Gibco), 100 μM nonessential amino acids (Gibco), 25 mM Hepes (pH 7.2) (Gibco), and 2 μg/mL polymyxin B (Gibco). Cell suspensions were seeded into 96-well plates at a density of 1.1×10^6 cells/mL. Titrating concentrations of recombinant SEB were added to cells and incubated for 18 h at 37 °C with 5% CO_2. Supernatants were assayed for IL-2 by enzyme-linked immunosorbent assay (ELISA) according to the manufacturer's instructions (Thermo Fisher Scientific). For flow cytometry, cells were dual stained with phycoerythrin (PE)-conjugated anti-CD25 (clone PC61.5) (eBioscience) and fluorescein isothiocyanate (FITC)-conjugated anti-Vβ8 (clone KJ16) (eBioscience). Events were acquired using a FACSCanto II (BD Biosciences), and data were analyzed using FlowJo version 10.7.1 (TreeStar).

Staphylococcal Bacteremia Model. Single bacterial colonies were picked from a TSA plate and grown in 3 mL TSB overnight (16 to 18 h). Cells were subsequently subcultured in TSB to an OD_{600} (optical density at 600 nm wavelength) of 0.1 and grown to postexponential phase (OD_{600} ~3.0 to 3.5). The bacterial pellet was washed once and resuspended in Hank's balanced salt solution (HBSS) to an OD_{600} of 0.15 for strain COL and 0.1 for strain MW2, corresponding to ~5×10^7 CFU/mL. Mice were injected via the tail vein with 5×10^6 CFU of *S. aureus* in a total volume of 100 μL. Mice were weighed and monitored daily. At various time points postinfection, mice were killed (maximum of 3 and 4 d for MW2 and COL, respectively), and the kidneys and liver were aseptically harvested. All organs were homogenized, plated on mannitol salt agar (Difco), and incubated at 37 °C overnight. *S. aureus* colonies were enumerated the following day with a limit of detection determined to be 3 CFU per 10 μL.

Antibody Depletion Protocols. $CD4^+$ and $CD8^+$ T cells were depleted in animals according to a protocol described previously (23). Briefly, mice were injected with 300 μg of T cell–depleting antibodies (anti-CD4 [clone GK1.5, BioXCell], anti-CD8 [clone YTS169.4, BioXCell], or both at 150 μg each) or isotype antibody control (clone LTF-2, BioXCell) 7, 6, and 1 d before infection with *S. aureus*. For IL-17A depletion, mice were injected with a 200-μg dose of anti–IL-17A mAb (clone 17F3; BioXCell) or a mouse IgG1 isotype antibody control (clone MOPC-21, BioXCell) 3 h before *S. aureus* infection, then with a further 100-μg dose 1 h after infection, as described previously (28). For IL-10 and IFN-γ depletions, mice were treated with a 250-μg dose of anti–IL-10 mAb (clone JES5-2A5), anti–IFN-γ (clone XMG1.2, BioXCell), or Rat IgG1 isotype antibody control, anti-horseradish peroxidase (clone HRPN), 18 h prior to infection. NK cells were depleted in mice with 200 μg of anti-NK1.1 mAb (clone PK136, BioXCell) or mouse IgG2a isotype antibody control (clone Cl.18, BioXCell) administered 18 h prior to infection, as described previously (55). All antibody doses were prepared in 100 to 200 μL PBS and administered by intraperitoneal (i.p.) injection.

Detection of Cytokines and Chemokines In Vivo. At various time points postinfection, serum supernatants and livers were collected. Supernatants were obtained from whole livers by homogenization in HBSS supplemented with the complete protease inhibitor mixture (Roche). Samples were analyzed using Mouse Cytokine Array/Chemokine Array 44-Plex (MD44, Eve Technologies). AST levels were assessed from murine serum using a mouse AST ELISA Kit (Abcam).

IFN-γ Treatment of Mice during *S. aureus* Bacteremia. DR4-B6 animals were infected with *S. aureus* COL Δ*seb* intravenously (i.v.) at a dose of 5×10^6 CFU in 100 μL of HBSS prepared as described in the staphylococcal bactermia model section. At 2 h before and 1 h after infection, animals were treated with 20 μg recombinant murine IFN-γ (Sino Biological) in 100 μL PBS by i.p. injection (40 μg total). Control animals were treated with PBS only. Animals were monitored daily and killed at 96 hpi to harvest livers. Bacterial burden was determined as described in the staphylococcal bactermia model section.

Flow Cytometry Analysis of Murine Cells. Livers were extracted from mice and pushed through a 0.7-μm cell strainer. Leukocytes were isolated from livers using a 33.75% Percoll gradient (GE Healthcare). Following isolation, red blood cells were lysed using ACK lysis buffer (Gibco) and washed with PBS containing 2% FBS. Following isolation, cells were stained and analyzed as outlined in *SI Appendix, SI Materials and Methods*.

Macrophage Depletion in Mice. Macrophage depletion was based on a protocol previously described (56). Briefly, 200 μL Clodronate containing liposomes and control liposomes (Clodrosome + Encapsome [Encapsula Nano Sciences]) were administered to the mice i.p. 2 d and 4 h prior to infection with bacteria. At 18 h prior to infection, IFN-γ–depleting or control antibodies were also administered to the mice.

Detection of Human Cytokines from Stimulated Human Cells. The ability of human cells to produce cytokines was determined from stimulated PBMCs. These cells were isolated from human blood by density-based centrifugation

MICROBIOLOGY

following layering of the blood onto Ficoll-Hypaque plus (GE healthcare). Cells were isolated and washed three times in RPMI (Gibco) and then resuspended in cRPMI. Cell suspension was seeded into 96-well plates to a final concentration of 1.0×10^6 cells/mL. Titrating concentrations of recombinant proteins or *S. aureus* supernatants were added to cells and incubated for 18 h at 37 °C with 5% CO_2. Supernatants were assayed for IL-2 or IFN-γ by ELISA according to the manufacturer's instructions (Thermo Fisher Scientific).

Macrophage Cultures and Infections. RAW 264.7 (a murine macrophage cell line) cells were maintained in RPMI 1640 supplemented with 10% FBS and grown in 12-well plates with coverslips for experimental analysis. Primary human macrophages were derived from blood monocytes isolated from healthy human volunteers as previously described (32, 57). Briefly, mononuclear cells were isolated from blood with lympholyte-poly (Cedarlane Laboratories) according to the manufacturer's instructions. Monocytes adhered to glass coverslips in 12-well plates (1.5×10^6 cells/well) and were subsequently cultured for 7 to 9 d in RPMI (Gibco) with 10% FBS (Wisent) and 0.5 ng/mL recombinant human macrophage colony-stimulating factor (M-CSF) (R&D Systems) to allow for differentiation of monocytes into macrophages. After 5 d of differentiation, adhered cells were washed with PBS and the medium was replaced with fresh RPMI + 10% FBS containing M-CSF. Macrophages were differentiated until day 7 and used experimentally until day 10.

For murine bone–derived macrophages, DR4-B6 mice were killed and leg bones were harvested for bone-marrow extraction. Bone marrow was flushed from the bones and washed with PBS prior to resuspension in RPMI supplemented with 5% FBS. Bone marrow–derived cells were adhered to glass coverslips in 12-well plates in a similar manner to human cells and stimulated with 10 ng/mL of murine M-CSF. Macrophages again were differentiated until day 7 and used experimentally until day 10.

Experimental infections for each type of macrophage followed the same protocol. *S. aureus* strains COL and MW2 were cultured overnight in TSB and then pelleted and resuspended in serum-free RPMI and diluted in serum-free RPMI to an OD_{600} of 0.5. Cells were infected with a multiplicity of infection (MOI) of 30 and, following inoculation, were centrifuged at $277 \times g$ for 2 min and then incubated for 30 min at 37 °C in the presence of 5% CO_2. Following phagocytosis, cells were treated with RPMI containing gentamicin (100 μg/mL) for 1 h at 37 °C to kill extracellular bacteria. Gentamicin was confirmed to be effective by plating supernatant of treatments onto TSA. Furthermore, minimal inhibitory concentration (MIC) for gentamicin with *S. aureus* MW2 was found to be 125 ng/mL, and for *S. aureus* COL, this value was below 62.5 ng/mL. After gentamicin treatment, macrophages were rinsed with PBS and incubated further in RPMI containing 10% FBS without antibiotic. At this point, recombinant human or murine IFN-γ (R&D Systems) was added at varying concentrations. Macrophages were incubated for 24 or 48 h following infection with *S. aureus* MW2 or COL, respectively, for derived macrophages or 12 or 24 h for infected RAW 264.7 cells. Enumeration of antibiotic-protected bacteria (i.e., intracellular bacteria) was performed by lysing infected macrophages with 0.1% (vol/vol) Triton X-100 in PBS. Macrophage lysates were serially diluted and plated on TSA for enumeration.

Statistical Analysis. All statistical analyses were performed using GraphPad Prism 9, and a P value <0.05 was considered statistically significant. For all bacterial burden CFU, analysis was performed with the nonparametric Mann–Whitney U test or Kruskal–Wallis test with an uncorrected Dunn's test for multiple comparisons, depending on group numbers. Flow cytometry data were analyzed using Welch's t test to determine significant differences between means of the isotype antibody and IFN-γ–depleted groups.

For the multiplex cytokine analysis heat map shown in Fig. 5*D*, each raw data point was normalized to a sample taken from an uninfected control animal that was killed at the same time point after treatment with the same antibody. Following normalization, the data from analysis at each time point were compared for statistical significance between the isotype antibody and IFN-γ depletion using a Student's t test. All significant values were extracted, and the mean quantity of the cytokine/chemokine detected in the isotype antibody–treated animals was divided by the quantity detected in the IFN-γ–depleted group. These values were converted to $\log_{10}$ values to give fold change in positive and negative values that could be plotted on a heat map.

For the human cytokine analysis performed in Fig. 7 *A–C*, the area under each curve for each donor was determined. These values were then compared using a paired t test or paired Friedman test for multiple comparisons, depending on the number of groups. Paired tests were used due to the large variation observed between individual human donors.

Data Availability. All study data are included in the article and/or *SI Appendix*.

ACKNOWLEDGMENTS. This work was supported by an operating grant from the Canadian Institutes of Health Research (CIHR) (PJT-166050) to S.W.T. and J.K.M. D.E.H. acknowledges funding from CIHR Grant PJT-153308, and S.M.K. acknowledges funding from CIHR Grant PJT-175070. Figs. 3*A*, 6*B*, and 7 *D* and *G* were created using Biorender.com.

1. S. Y. C. Tong, J. S. Davis, E. Eichenberger, T. L. Holland, V. G. Fowler Jr., *Staphylococcus aureus* infections: Epidemiology, pathophysiology, clinical manifestations, and management. *Clin. Microbiol. Rev.* **28**, 603–661 (2015).
2. J. M. Kwiecinski, A. R. Horswill, *Staphylococcus aureus* bloodstream infections: Pathogenesis and regulatory mechanisms. *Curr. Opin. Microbiol.* **53**, 51–60 (2020).
3. K. A. Corl *et al.*, Delay in antibiotic administration is associated with mortality among septic shock patients with *Staphylococcus aureus* bacteremia. *Crit. Care Med.* **48**, 525–532 (2020).
4. N. A. Turner *et al.*, Methicillin-resistant *Staphylococcus aureus*: An overview of basic and clinical research. *Nat. Rev. Microbiol.* **17**, 203–218 (2019).
5. T. J. Foster, J. A. Geoghegan, V. K. Ganesh, M. Höök, Adhesion, invasion and evasion: The many functions of the surface proteins of *Staphylococcus aureus. Nat. Rev. Microbiol.* **12**, 49–62 (2014).
6. J. Josse, F. Laurent, A. Diot, Staphylococcal adhesion and host cell invasion: Fibronectin-binding and other mechanisms. *Front. Microbiol.* **8**, 2433 (2017).
7. K. J. Koymans, M. Vrieling, R. D. Gorham, J. A. G. van Strijp, "Staphylococcal immune evasion proteins: Structure, function, and host adaptation" in *Staphylococcus aureus: Microbiology, Pathology, Immunology, Therapy and Prophylaxis*, F. Bagnoli, R. Rappuoli, G. Grandi, Eds. (Springer International Publishing, Cham, 2017), pp. 441–489.
8. F. Alonzo III, V. J. Torres, The bicomponent pore-forming leucocidins of *Staphylococcus aureus. Microbiol. Mol. Biol. Rev.* **78**, 199–230 (2014).
9. B. J. Berube, J. Bubeck Wardenburg, *Staphylococcus aureus* α-toxin: Nearly a century of intrigue. *Toxins (Basel)* **5**, 1140–1166 (2013).
10. S. W. Tuffs, S. M. M. Haeryfar, J. K. McCormick, Manipulation of innate and adaptive immunity by staphylococcal superantigens. *Pathogens* **7**, 53 (2018).
11. A. R. Spaulding *et al.*, Staphylococcal and streptococcal superantigen exotoxins. *Clin. Microbiol. Rev.* **26**, 422–447 (2013).
12. G. J. Wilson *et al.*, A novel core genome-encoded superantigen contributes to lethality of community-associated MRSA necrotizing pneumonia. *PLoS Pathog.* **7**, e1002271 (2011).
13. S. W. Tuffs *et al.*, The *Staphylococcus aureus* superantigen SEIX is a bifunctional toxin that inhibits neutrophil function. *PLoS Pathog.* **13**, e1006461 (2017).
14. W. Salgado-Pabón *et al.*, Superantigens are critical for *Staphylococcus aureus* infective endocarditis, sepsis, and acute kidney injury. *mBio* **4**, e00494-13 (2013).
15. S. X. Xu *et al.*, Superantigens subvert the neutrophil response to promote abscess formation and enhance *Staphylococcus aureus* survival in vivo. *Infect. Immun.* **82**, 3588–3598 (2014).
16. S. X. Xu, K. J. Kasper, J. J. Zeppa, J. K. McCormick, Superantigens modulate bacterial density during *Staphylococcus aureus* nasal colonization. *Toxins (Basel)* **7**, 1821–1836 (2015).
17. M. Vrieling *et al.*, Population analysis of *Staphylococcus aureus* reveals a cryptic, highly prevalent superantigen SEIW that contributes to the pathogenesis of bacteremia. *mBio* **11**, e02082-20 (2020).
18. S. R. Gill *et al.*, Insights on evolution of virulence and resistance from the complete genome analysis of an early methicillin-resistant *Staphylococcus aureus* strain and a biofilm-producing methicillin-resistant Staphylococcus epidermidis strain. *J. Bacteriol.* **187**, 2426–2438 (2005).
19. B. L. Rellahan, L. A. Jones, A. M. Kruisbeek, A. M. Fry, L. A. Matis, In vivo induction of anergy in peripheral V beta 8+ T cells by staphylococcal enterotoxin B. *J. Exp. Med.* **172**, 1091–1100 (1990).
20. P. D. Fey *et al.*, Comparative molecular analysis of community- or hospital-acquired methicillin-resistant *Staphylococcus aureus. Antimicrob. Agents Chemother.* **47**, 196–203 (2003).
21. J. M. King, K. Kulhankova, C. S. Stach, B. G. Vu, W. Salgado-Pabón, Phenotypes and virulence among *Staphylococcus aureus* USA100, USA200, USA300, USA400, and USA600 clonal lineages. *mSphere* **1**, e00071-16 (2016).
22. K. J. Kasper *et al.*, Bacterial superantigens promote acute nasopharyngeal infection by *Streptococcus pyogenes* in a human MHC class II-dependent manner. *PLoS Pathog.* **10**, e1004155 (2014).
23. J. J. Zeppa *et al.*, Nasopharyngeal infection by *Streptococcus pyogenes* requires superantigen-responsive Vβ-specific T cells. *Proc. Natl. Acad. Sci. U.S.A.* **114**, 10226–10231 (2017).
24. P. A. Szabo *et al.*, Invariant natural killer T cells are pathogenic in the HLA-DR4-transgenic humanized mouse model of toxic shock syndrome and can be targeted to reduce morbidity. *J. Infect. Dis.* **215**, 824–829 (2017).
25. S. Xu, X. Cao, Interleukin-17 and its expanding biological functions. *Cell. Mol. Immunol.* **7**, 164–174 (2010).
26. S. Naundorf *et al.*, IL-10 interferes directly with TCR-induced IFN-gamma but not IL-17 production in memory T cells. *Eur. J. Immunol.* **39**, 1066–1077 (2009).

27. A. Y. Tilahun, M. Holz, T.-T. Wu, C. S. David, G. Rajagopalan, Interferon gamma-dependent intestinal pathology contributes to the lethality in bacterial superantigen-induced toxic shock syndrome. *PLoS One* **6**, e16764 (2011).
28. P. A. Szabo *et al.*, Rapid and rigorous IL-17A production by a distinct subpopulation of effector memory T lymphocytes constitutes a novel mechanism of toxic shock syndrome immunopathology. *J. Immunol.* **198**, 2805–2818 (2017).
29. A. N. Spaan, B. G. J. Surewaard, R. Nijland, J. A. G. van Strijp, Neutrophils versus *Staphylococcus aureus*: A biological tug of war. *Annu. Rev. Microbiol.* **67**, 629–650 (2013).
30. G. R. Pidwill, J. F. Gibson, J. Cole, S. A. Renshaw, S. J. Foster, The role of macrophages in *Staphylococcus aureus* infection. *Front. Immunol.* **11**, 620339 (2021).
31. L. Leder *et al.*, A mutational analysis of the binding of staphylococcal enterotoxins B and C3 to the T cell receptor beta chain and major histocompatibility complex class II. *J. Exp. Med.* **187**, 823–833 (1998).
32. R. S. Flannagan, B. Heit, D. E. Heinrichs, Intracellular replication of *Staphylococcus aureus* in mature phagolysosomes in macrophages precedes host cell death, and bacterial escape and dissemination. *Cell. Microbiol.* **18**, 514–535 (2016).
33. W. Salgado-Pabón, P. M. Schlievert, Models matter: The search for an effective *Staphylococcus aureus* vaccine. *Nat. Rev. Microbiol.* **12**, 585–591 (2014).
34. R. M. McLoughlin, J. C. Lee, D. L. Kasper, A. O. Tzianabos, IFN-γ regulated chemokine production determines the outcome of *Staphylococcus aureus* infection. *J. Immunol.* **181**, 1323–1332 (2008).
35. T. Aoyama, S. Inokuchi, D. A. Brenner, E. Seki, CX3CL1-CX3CR1 interaction prevents carbon tetrachloride-induced liver inflammation and fibrosis in mice. *Hepatology* **52**, 1390–1400 (2010).
36. C. J. Horras, C. L. Lamb, K. A. Mitchell, Regulation of hepatocyte fate by interferon-γ. *Cytokine Growth Factor Rev.* **22**, 35–43 (2011).
37. B. G. J. Surewaard *et al.*, Identification and treatment of the *Staphylococcus aureus* reservoir in vivo. *J. Exp. Med.* **213**, 1141–1151 (2016).
38. B. G. J. Surewaard *et al.*, α-Toxin induces platelet aggregation and liver injury during *Staphylococcus aureus* sepsis. *Cell Host Microbe* **24**, 271–284.e3 (2018).
39. S. K. Jorch *et al.*, Peritoneal GATA6+ macrophages function as a portal for *Staphylococcus aureus* dissemination. *J. Clin. Invest.* **129**, 4643–4656 (2019).
40. S. M. Larkin, D. N. Williams, M. T. Osterholm, R. W. Tofte, Z. Posalaky, Toxic shock syndrome: Clinical, laboratory, and pathologic findings in nine fatal cases. *Ann. Intern. Med.* **96**, 858–864 (1982).
41. A. F. Brown *et al.*, Memory Th1 cells are protective in invasive *Staphylococcus aureus* infection. *PLoS Pathog.* **11**, e1005226 (2015).
42. Y. X. Zhao, I. M. Nilsson, A. Tarkowski, The dual role of interferon-γ in experimental *Staphylococcus aureus* septicaemia versus arthritis. *Immunology* **93**, 80–85 (1998).
43. K. E. Rudd *et al.*, Global, regional, and national sepsis incidence and mortality, 1990-2017: Analysis for the Global Burden of Disease Study. *Lancet* **395**, 200–211 (2020).
44. E. C. Van Der Slikke, A. Y. An, R. E. W. Hancock, H. R. Bouma, Exploring the pathophysiology of post-sepsis syndrome to identify therapeutic opportunities. *EBioMedicine* **61**, 103044 (2020).
45. R. S. Hotchkiss, G. Monneret, D. Payen, Immunosuppression in sepsis: A novel understanding of the disorder and a new therapeutic approach. *Lancet Infect. Dis.* **13**, 260–268 (2013).
46. C. R. Romero *et al.*, The role of interferon-γ in the pathogenesis of acute intra-abdominal sepsis. *J. Leukoc. Biol.* **88**, 725–735 (2010).
47. M. Nalos *et al.*, Immune effects of interferon gamma in persistent staphylococcal sepsis. *Am. J. Respir. Crit. Care Med.* **185**, 110–112 (2012).
48. D. Payen *et al.*, Multicentric experience with interferon gamma therapy in sepsis induced immunosuppression. A case series. *BMC Infect. Dis.* **19**, 1–10 (2019).
49. H. Karauzum *et al.*, Lethal CD4 T cell responses induced by vaccination against *Staphylococcus aureus* bacteremia. *J. Infect. Dis.* **215**, 1231–1239 (2017).
50. V. G. Fowler *et al.*, Effect of an investigational vaccine for preventing *Staphylococcus aureus* infections after cardiothoracic surgery: A randomized trial. *JAMA* **309**, 1368–1378 (2013).
51. T. Bae, O. Schneewind, Allelic replacement in *Staphylococcus aureus* with inducible counter-selection. *Plasmid* **55**, 58–63 (2006).
52. I. R. Monk, J. J. Tree, B. P. Howden, T. P. Stinear, T. J. Foster, Complete bypass of restriction systems for major *Staphylococcus aureus* lineages. *mBio* **6**, e00308–e00315 (2015).
53. I. R. Monk, I. M. Shah, M. Xu, M.-W. Tan, T. J. Foster, Transforming the untransformable: Application of direct transformation to manipulate genetically *Staphylococcus aureus* and *Staphylococcus epidermidis*. *mBio* **3**, e00277-11 (2012).
54. T. A. Chau *et al.*, Toll-like receptor 2 ligands on the staphylococcal cell wall downregulate superantigen-induced T cell activation and prevent toxic shock syndrome. *Nat. Med.* **15**, 641–648 (2009).
55. J. L. Hayworth *et al.*, CD1d-independent activation of mouse and human iNKT cells by bacterial superantigens. *Immunol. Cell Biol.* **90**, 699–709 (2012).
56. J. Stritzker *et al.*, Enterobacterial tumor colonization in mice depends on bacterial metabolism and macrophages but is independent of chemotaxis and motility. *Int. J. Med. Microbiol.* **300**, 449–456 (2010).
57. R. S. Flannagan *et al.*, Burkholderia cenocepacia disrupts host cell actin cytoskeleton by inactivating Rac and Cdc42. *Cell. Microbiol.* **14**, 239–254 (2012).